

Available online at [www.sciencedirect.com](http://www.sciencedirect.com)

ScienceDirect

journal homepage: [www.elsevier.com/locate/burns](http://www.elsevier.com/locate/burns)

# Evaluating clinical observation versus Spatial Frequency Domain Imaging (SFDI), Laser Speckle Imaging (LSI) and thermal imaging for the assessment of burn depth

Adrien Ponticorvo<sup>a</sup>, Rebecca Rowland<sup>a</sup>, Melissa Baldado<sup>a</sup>,  
David M. Burmeister<sup>b</sup>, Robert J. Christy<sup>b</sup>, Nicole P. Bernal<sup>c</sup>,  
Anthony J. Durkin<sup>a,d,\*</sup>

<sup>a</sup> Beckman Laser Institute and Medical Clinic, University of California, 1002 Health Sciences Road East, Irvine, CA 92617, United States

<sup>b</sup> United States Army Institute of Surgical Research, 3650 Chambers Pass, Fort Sam Houston, TX, 78234, United States

<sup>c</sup> UC Irvine Regional Burn Center, Department of Surgery, 333 City Boulevard West, Suite 705, Orange, CA 92868, United States

<sup>d</sup> Department of Biomedical Engineering, University of California, 3120 Natural Sciences II, Irvine, CA 92697, United States

## ARTICLE INFO

Article history:

Accepted 13 September 2018

## ABSTRACT

While clinical examination is needed for burn severity diagnosis, several emerging technologies aim to quantify this process for added objectivity. Accurate assessments become easier after burn progression, but earlier assessments of partial thickness burn depth could lead to earlier excision and grafting and subsequent improved healing times, reduced rates of scarring/infection, and shorter hospital stays. Spatial Frequency Domain Imaging (SFDI), Laser Speckle Imaging (LSI) and thermal imaging are three non-invasive imaging modalities that have some diagnostic ability for noninvasive assessment of burn severity, but have not been compared in a controlled experiment. Here we tested the ability of these imaging techniques to assess the severity of histologically confirmed graded burns in a swine model. Controlled, graded burn wounds, 3 cm in diameter were created on the dorsum of Yorkshire pigs (n=3, 45–55 kg) using a custom-made burn tool that ensures consistent pressure has been employed by various burn research groups. For each pig, a total of 16 burn wounds were created on the dorsal side. Biopsies were taken for histological analysis to verify the severity of the burn. Clinical analysis, SFDI, LSI and thermal imaging were performed at 24 and 72 h after burn to assess the accuracy of each imaging technique. In terms of diagnostic accuracy, using histology as a reference, SFDI (85%) and clinical analysis (83%) performed significantly better than LSI (75%) and thermography (73%) 24 h after the burn. There was no statistically significant improvement from 24 to 72 h across the different imaging modalities. These data indicate that these imaging modalities, and specifically SFDI, can be added to the burn clinicians' toolbox to aid in early assessment of burn severity.

© 2018 Elsevier Ltd and ISBI. All rights reserved.

\* Corresponding author at: Department of Biomedical Engineering, University of California, 3120 Natural Sciences II, Irvine, 92697 CA, United States.

E-mail address: [adurkin@uci.edu](mailto:adurkin@uci.edu) (A.J. Durkin).

<https://doi.org/10.1016/j.burns.2018.09.026>

0305-4179/© 2018 Elsevier Ltd and ISBI. All rights reserved.

---

## 1. Introduction

There are as many as 11 million cases worldwide annually of people with medical attention due to burn injuries [1]. Burn wounds and the subsequent scarring that can result from these injuries are damaging both cosmetically and functionally, necessitating the search for better and more efficient treatments. One immediate way to both improve treatment/outcomes and reduce overall costs related to patient care is to make accurate diagnoses earlier. Delays decision making related to excision and grafting enables burn wound progression [2] and increases length of hospital stay. This gap in health care has led to the development of numerous imaging technologies that have potential for assisting physicians in rapidly and correctly diagnosing burn severity.

Laser Doppler based techniques have been used since the 1980s to assess perfusion in burns alongside clinical evaluation [3]. Laser speckle imaging (LSI) [4,5], also known as Laser Speckle Contrast Analysis (LASCA) [6], utilizes similar principles to generate perfusion images over a large field of view with fast acquisition times making it ideally suited to study perfusion in burns. Measurements that indicate low blood perfusion may imply the destruction of the underlying vasculature and indicate a need for surgical intervention, while high perfusion measurements suggest that the vascular network is intact and there is a strong chance of spontaneous healing. While several studies have shown that LSI is more accurate than clinical analysis for burn assessment, this accuracy is a highly time dependent phenomenon. It is still common to wait 48–72h before excision to ensure accurate clinical observation of burn depth [3]. Other studies have employed laser Doppler measurements earlier than 48h with inconclusive results [7].

Thermal imaging has recently been adapted for burn wound diagnostics [4]. In relation to burn wound severity, it is typically used to identify regions of tissue within a burn that demonstrate reduced surface temperature relative to some baseline normal skin surface temperature. The reduction in temperature suggests that in these areas, the underlying blood vessels have been damaged to the point where the lack of perfusion leads to a reduction in thermal emission and this can be empirically related to burn depth [8–10]. Recent studies suggest that thermography is only as accurate as photographic clinical assessments, and is highly dependent on the ambient temperature during measurements [4]. Other studies have found that LSI outperforms thermal imaging in a clinical setting [8]. However, one difficulty in assessing these imaging techniques in a clinical environment is that “ground truth” is not known.

Multispectral and hyperspectral imaging have also been investigated within the context of assessment of burn wound severity. These techniques utilize images taken at multiple wavelengths of light to measure the reflectance from burn tissue [11,12]. These reflectance measurements can be converted into concentrations of chromophores such oxygenated and deoxygenated hemoglobin, but require assumptions about the reduced scattering coefficient [13,14]. Differences in oxygenated and deoxygenated hemoglobin concentrations of burn wound regions and unburned skin indicate damage to

the underlying vasculature which can be indicative of burn severity.

Spatial Frequency Domain Imaging (SFDI) is a developing imaging technique that can be used to determine the optical properties and chromophore concentrations of tissue [15–18]. It is sensitive to both hemodynamic [19,20] and structural [21–23] components in tissue. Our previous research suggests that SFDI can be used to noninvasively characterize changes in tissue structure and function over a range of burn grades in rats and pigs [21–23]. In the porcine burn study, we found that changes in tissue scattering properties are acutely related to structural damage to collagen (i.e., the zone of coagulation). While our previous SFDI imaging of burn severity in a porcine model used a device based on 3 near infrared LED wavelengths [21], here we employ a new SFDI device based on 9 wavelengths over the range 471nm–971nm. Specifically, we compare the histologically validated burn severity prediction accuracy of SFDI, LSI and thermal imaging, to clinical impression. We examined the performance of these techniques within the context of a swine model of graded burn wounds.

---

## 2. Methodology

### 2.1. Porcine model

All experiments were performed in accordance with the UC Irvine Institutional Animal Care and Use Committee (IACUC protocol #2015-3154). Three Yorkshire pigs (50kg average weight) were used in this experiment. Animals were allowed to acclimate to their individual housing for 7 days prior to the experiment. An intramuscular injection of tiletamine-zolazepam (Telazol, 6mg/kg) was used to sedate the animals. Hair was removed from the area of interest with clippers. Animals were intubated and placed on an automatic ventilator with an initial tidal volume at 10ml/kg, peak pressure at 20 cmH<sub>2</sub>O and respiration rate at 10 breaths per minute. The ventilator setting was adjusted to maintain an end tidal PCO<sub>2</sub> of 38–42mmHg, and anesthesia was maintained at 1–3% isoflurane. Vital signs were continuously monitored and kept constant by adjusting anesthesia levels. A heating blanket was used to maintain a constant body temperature (36–38°C). Controlled, graded burn wounds were created using a custom-made setup described previously [21]. Briefly, custom made cylindrical brass probes (3cm diameter) with stainless steel posts were custom fabricated along with a spring loaded device to hold the probes and ensure consistent pressure. The brass probes were heated in a dry bath incubator to 100°C and held in place by a custom made aluminum block. Sixteen burns were created along the dorsal side approximately 1cm from the spine and approximately 3cm away from each other. 8 wounds were created on each side of the spine, with contact times of 5, 10, 15, 20, 25, 30, 35, and 40s. Non-adherent gauze (Telfa, Tyco Healthcare, Mansfield, MA) was placed on top of the wound and held in place with Ioban™ (3M, St. Paul, MN). Bandaging materials were removed at 24h and 72h after the initial burn in order to image the wounds. Pigs were survived for 28 days in order to evaluate burn healing and relate this back to the original assessment of the burn. A diagram of the animal setup is shown in Fig. 1a.

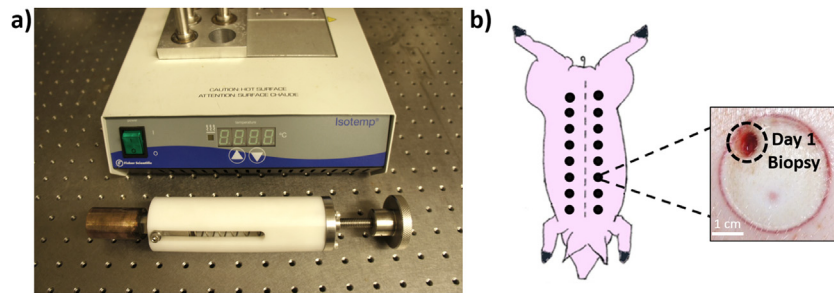


**Fig. 1 – a) Isotemp™ dry bath incubator (Thermo Fisher Scientific Inc., Pittsburgh, PA) and custom spring loaded burn device. b) A description of the burn placement and typical burn size and biopsy location.**

## 2.2. Histological assessment

Histological assessments were performed during the experiment to determine the true burn severity. At 24h after the initial burn injury, a 6mm punch biopsy was used to collect tissue from within each burn region near the edge of the burn (Fig. 1b). This biopsy was performed after all of the appropriate imaging was completed. Great care was taken to ensure that biopsy only contained tissue from the burn region. We have considerable practice with this approach in previous work [21,22]. In addition, the biopsy region was selected in the most homogenous appearing area near the edge. Biopsies were fixed in 10% neutral buffered formalin for 48h, dehydrated in alcohol, and embedded in paraffin wax. The biopsies were sectioned into 7  $\mu\text{m}$  thick samples and stained with Masson's Trichrome (ab150686, Abcam, Cambridge, MA), marking healthy collagen blue, and damaged collagen, epidermis, and muscle tissue hair follicle lumens red. To determine burn depth and categorize the burn, the mounted tissue sections were examined for collagen coagulation and hair follicle damage [24,25]. Burns were either categorized as benefiting or not benefiting from surgical excision and grafting based on the depth of coagulation and the damage to hair follicles and vessels. When damage in these areas did not exceed the thickness of the epidermis or the damage was restricted to the papillary dermis, the burn was classified as one that would heal without surgical intervention. Damage that extended through to the reticular dermis indicated a burn that would typically benefit from surgical intervention, although no intervention was performed. The percent of dermal damage was measured by comparing the depth of thermal damage to the overall depth of the dermis. The results of this histological analysis were used as the gold standard assessment of burn depth.

## 2.3. Clinical assessment

A board certified (surgery and critical care) burn surgeon with 15 years of experience assessed the severity of each burn at 24 and 72h after the initial injury in order to similarly categorize whether the burns would benefit from a graft. Importantly, no surgical intervention (i.e., excision/grafting) was performed on these wounds in order to allow for inspection at subsequent time points. Time points were chosen to represent a time frame that spans an ideal and realistic period for excision and

grafting [3]. The surgeon was instructed to utilize any visual or tactile clues that would normally be used to assess burn severity in a clinical patient. The area of the burn that would later be biopsied was also the focus of the clinical assessment.

## 2.4. Laser Speckle Imaging (LSI)

LSI data was collected using a PeriCam PSI system (Perimed AB, Sweden) at the 24 and 72h time points after the initial injury. The device was placed at a height of 25cm above the burn wound creating a field of view of  $15 \times 15\text{cm}$ . Images were collected at a rate of five images/second for 60s and then averaged. All image collection, region of interest (ROI) selection and analysis was done using the Perimed PimSoft v2 software that reported data in Perfusion Units (PU) [6].

## 2.5. Thermal imaging

Thermal images were collected with a FLIR A300 (FLIR Systems, Inc., Wilsonville, OR;  $7.5\text{--}13\mu\text{m}$ ) at the 24 and 72h time points after the initial injury. The device was placed at a height of 40cm above the burn wound creating a field of view of  $17 \times 22\text{cm}$ . All image collection, ROI selection and analysis was done using FLIR Tools v5.13.17214.2001, which reported temperature values with a resolution of  $0.1^\circ\text{C}$  and an assumed emissivity of 0.98, previously validated in skin tissue [26].

## 2.6. Spatial Frequency Domain Imaging (SFDI)

The Reflect RS™ (Modulated Imaging, Inc., Irvine, CA), a commercially available SFDI measurement system capable of imaging optical properties (absorption coefficient,  $\mu_a$  and reduced scattering coefficient,  $\mu'_s$ ) [16] of tissue over large fields of view ( $20 \times 15\text{cm}$ ) was employed. The device was placed at a height of 32cm above the burn wound, and centered so each image captured two neighboring burns at a time. Imaging was performed through the MI Acquire v1.34.00 software. Each region of interest was imaged 3 consecutive times requiring a total of approximately 90s. Sinusoidal patterns are projected and images were captured at 8 wavelengths between 471nm–850nm and at 5 spatial frequencies evenly spaced between  $0\text{mm}^{-1}$  and  $0.2\text{mm}^{-1}$  according to a protocol that we have previously employed [21]. In addition planar (0 spatial frequency) reflectance images were acquired at each of the 8 spatially modulated wavelengths and at 971nm.

After each day of imaging, a reference calibration phantom having known optical properties was measured using the SFDI device under the same lighting conditions as the animal measurements, as has previously described in detail [15]. This phantom is made of a silicon based polymer, mixed with India ink and titanium dioxide, to mimic tissue optical properties [27]. The phantom and files of its optical properties are provided with the Reflect RS™ SFDI instrument. After all measurements were complete, the raw image files were processed in the MI-Analyze interface, part of the MI Acquire software package. Through this processing, the reflectance images were calibrated against the phantom measurements, and converted to images of the absorption and reduced scattering coefficient ( $\mu_s'$ ) at all measured wavelengths. A schematic of the imaging setup for all 3 instruments, a visualization of their projected illumination methods, and their output data is depicted in Fig. 2.

### 2.7. Color photography

Color images were acquired at a fixed distance and angle in relationship to the burn in order to ensure reproducibility. The color camera used here was a 14-megapixel digital camera (NEX-3, Sony Corporation of America, New York, NY) and was employed at the conclusion of each imaging session in order to document the clinical appearance of burn wounds at each time point.

### 2.8. Statistical analysis

For each imaging modality, a region of interest (ROI) approximately  $6 \times 6$  mm in size within the burn wound and

encompassing the entire biopsied region was selected so as to match the histological analysis of the biopsied region and the clinical assessment. Data sets from the different imaging devices were exported to Microsoft Excel (Microsoft Corporation, Redmond, WA) before statistical analysis was completed using R 3.4.3 (The R Foundation). A receiver operator curve (ROC) was generated for each imaging modality at the 24 and 72h time points, and the area under the curve (AUC) was calculated to determine the ability of each technique to correctly classify burns in a binary manner as either severe enough to benefit from a graft or not severe enough that a graft would be necessary. A p-value  $< 0.05$  testing the null hypothesis that the AUC=0.5 was considered significant. In order to compare results between different imaging modalities, McNemar's test was used with a p-value  $< 0.05$  considered significant. This statistical test determines if there are differences in paired binary data collected from matched subjects. In this case the binary data was the imaging modality determining if a burn wound would need a graft. The main outcome measure of the experiment was to compare the results of the different imaging modalities graded against the histological assessment, which was considered the "ground truth". The secondary outcome was to compare each of the different modalities at the 24 and 72h time points. The Youden index is a technique used to objectively determine the optimal threshold from an ROC curve [28]. This was used on each imaging modality to determine a threshold that would predict whether a particular imaging modality categorized the wound as needing a graft or not needing a graft. Each imaging modality then determined the accuracy, sensitivity, specificity, positive predictive values, negative predictive values at the 24 and 72h time points. Sensitivity was determined to be an imaging modality's ability

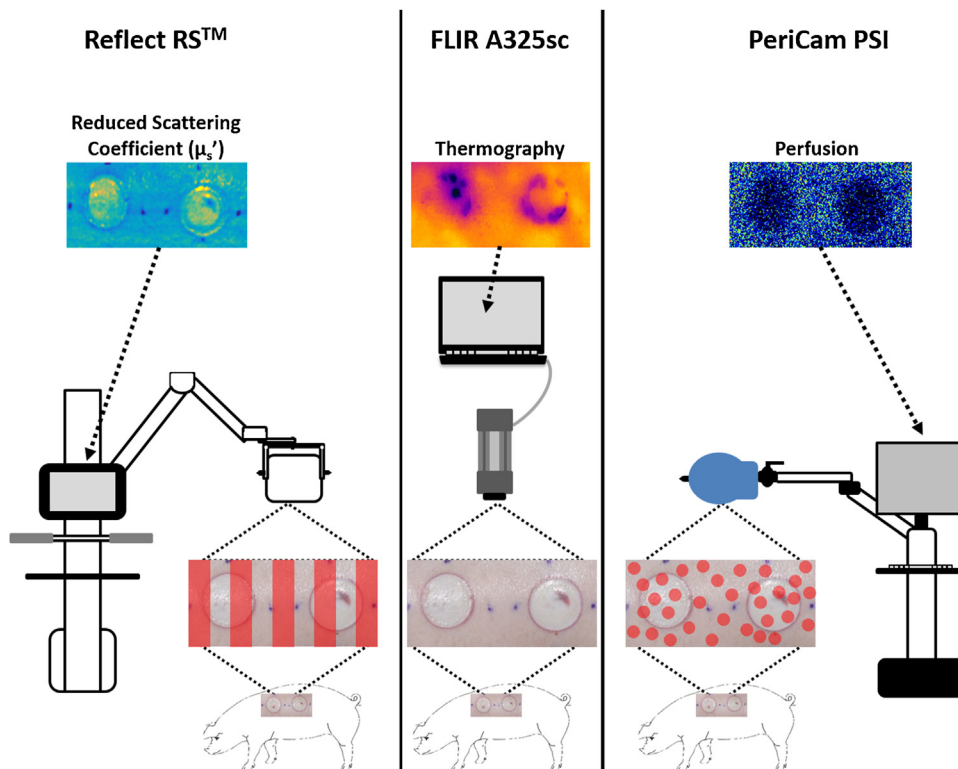


Fig. 2 – A schematic of the three imaging modalities used in the study. From left to right, SFDI, thermal imaging, and LSI.

to correctly determine if a burn wound received a graft when the histological analysis established that the burn wound would benefit from a graft. Specificity was determined to be an imaging modality's ability to correctly determine if a burn wound would not benefit from a graft when the histological analysis established that the burn would not benefit from a graft.

### 3. Results

#### 3.1. Histological assessment

Burn severity was determined by assessing each stained histologic sample at 24h. Burns were either categorized as undergoing or not undergoing surgical excision and grafting based on the depth of collagen coagulation and the damage to hair follicles, as seen in Fig. 3. When damage in these areas did not exceed the thickness of the epidermis or the damage was restricted to the papillary dermis, the burn was classified as one that would heal without surgical intervention. Damage that extended through to the reticular dermis or affected more than 50% of the reticular dermis indicated a burn that would typically undergo surgical intervention, although no intervention was performed. Using these criteria, 19 of the 48 burns included in the study would not benefit from surgical intervention, while 29 of the 48 burns were severe enough to benefit from surgical intervention. Table 1 breaks down the number of burns that were severe enough to undergo surgical intervention as a function of burn contact time and the average percent of dermal damage for each set of contact times.

#### 3.2. Clinical assessment

After the imaging sessions at 24h and 72h, a burn surgeon performed a clinical assessment of each wound to classify whether or not surgical intervention would be prescribed. This was compared to the histological assessment to determine

**Table 1 – Burns of various contact times listed with the percentage that would benefit from grafts based on histological analysis as well as the average percentage of dermal damage.**

Burn contact time (Seconds)	Histological assessment (Graft)	Average percent of dermal damage
5-10	0/12 (0%)	14.7%
15-20	5/12 (42%)	27.0%
25-30	7/12 (58%)	36.8%
35-40	12/12 (100%)	53.0%
Total	29/48 (60%)	

diagnostic accuracy. The surgeon was blinded by the randomization of burn contact times for each burn. Table 2 shows how the overall accuracy of the clinical assessment at 24 and 72h, as well as a breakdown of the accuracy for different groups of burn contact times. The 24h clinical assessments had an overall accuracy of 83% (correct classification of 40/48 burn wounds) with a sensitivity of 100% and a specificity of 58%. The positive and negative predictive values were 78% and 100% respectively. The 72h clinical assessments had an overall accuracy of 85% (correct classification of 41/48 burn wounds) with a sensitivity of 100% and a specificity of 63%. The positive and negative predictive values were 81% and 100% respectively. There was no statistically significant difference between the clinical assessments at 24h vs. 72h. The majority of the incorrect clinical assessments were made on burns with contact times of 15-20s.

#### 3.3. Laser Speckle Imaging

The averaged perfusion values at 24 and 72h, over the appropriate ROI, were used to create the ROC shown in Fig. 4a. The area under the curve (AUC) of the 24h perfusion

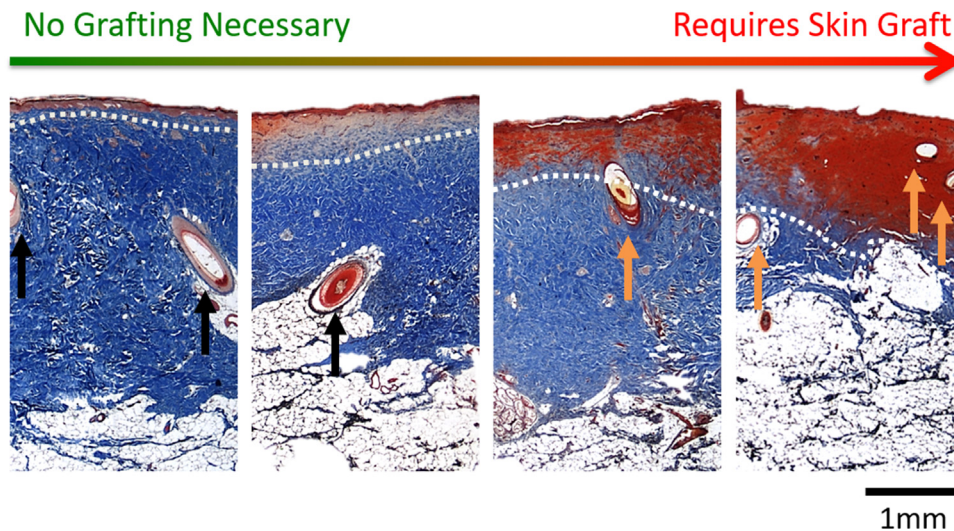


**Fig. 3 – Biopsies of 5, 15, 25, and 40s burns were taken at 24h and stained with Masson's Trichrome. The depth of denatured collagen is indicated by the white dotted line. Intact hair follicles are designated by black arrows, and damaged hair follicles are marked by orange arrows.**

**Table 2 – Correct clinical assessment of burns based on histological results.**

Burn contact time (Seconds)	24h assessment (Correct)	72h assessment (Correct)
5-10	10/12	11/12
15-20	7/12	7/12
25-30	11/12	11/12
35-40	12/12	12/12
Total	40 / 48	41 / 48

data was 0.79, while the AUC of the 72h perfusion data was 0.85. Both values were statistically significant ( $p < 0.001$ ). After choosing a threshold of 39.7 PU, the overall accuracy of the 24h perfusion values were 75% (correct classification of 36/48) with a sensitivity of 66% and a specificity of 90%. The positive and negative predictive values were 91% and 63% respectively. The overall accuracy of the 72h perfusion values was 83% (correct classification of 40/48) with a sensitivity of 100% and a specificity of 58%. The positive and negative predictive values

were 78% and 100% respectively. There was no statistically significant difference between the classifying ability of the perfusion values at 24h vs 72h. Fig. 4b shows typical perfusion images from 24 and 72h time points. Perfusion within the burn region is lower than perfusion for unburned tissue in all burn severities at 24h. While at 72h, perfusion in the periphery of the 5s burn is higher than unburned tissue, perfusion in the 20s, 25s, and 35s burns is still lower than unburned tissue by 72h (Fig. 4b).

**3.4. Thermal imaging**

The ROC curve for the temperature values collected via thermal imaging at 24 and 72h time points are shown in Fig. 5a. The AUC of the 24h thermography values was 0.76, while the AUC of the 72h thermography values was 0.79. Both values were statistically significant ( $p < 0.01$ ). After choosing a threshold of 34.9°C, the overall accuracy of the 24h thermography values were 73% (correct classification of 35/48) with a sensitivity of 66% and a specificity of 84%. The positive and negative predictive values were 86% and 61% respectively. The 72h thermography values had an overall accuracy of 75% (correct classification of 36/48) with a

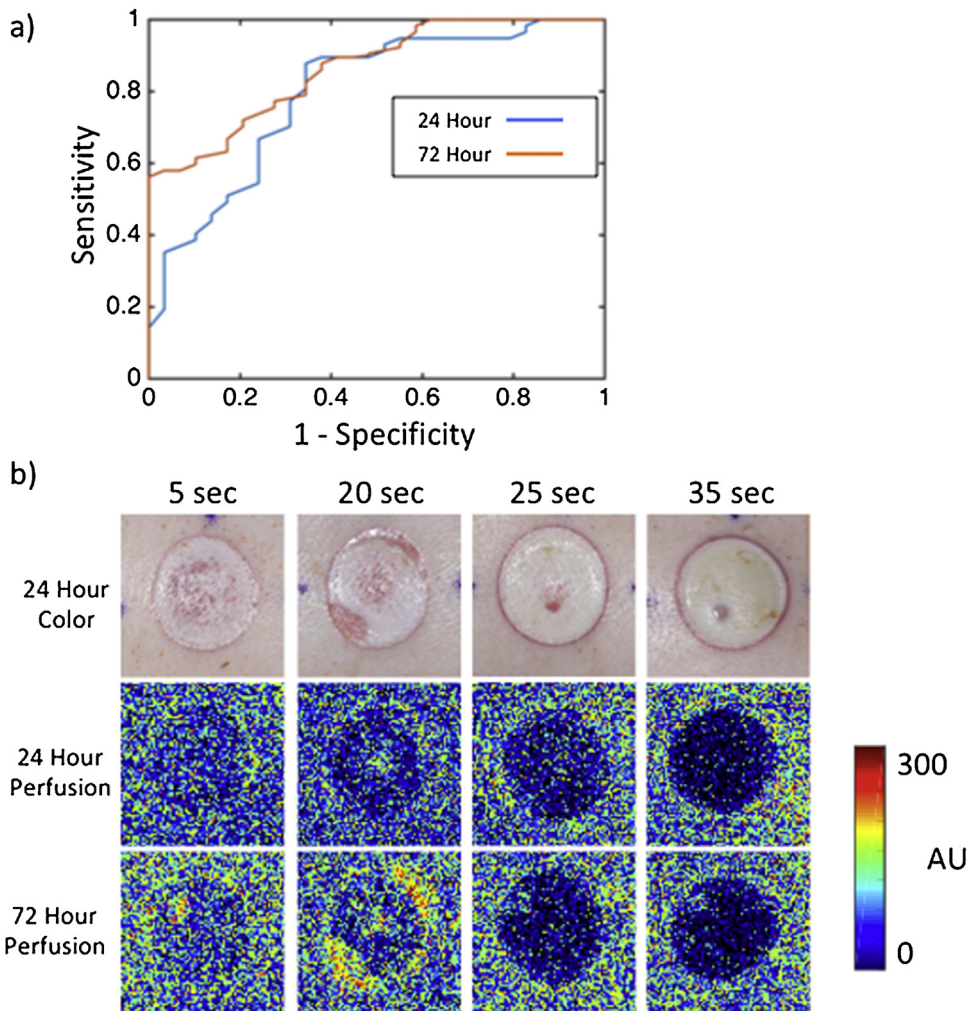


**Fig. 4 – a) ROC curves of LSI perfusion data at 24 and 72h after burn. b) Perfusion images from 5, 20, 25 and 35s burns at 24 and 72h after burn.**

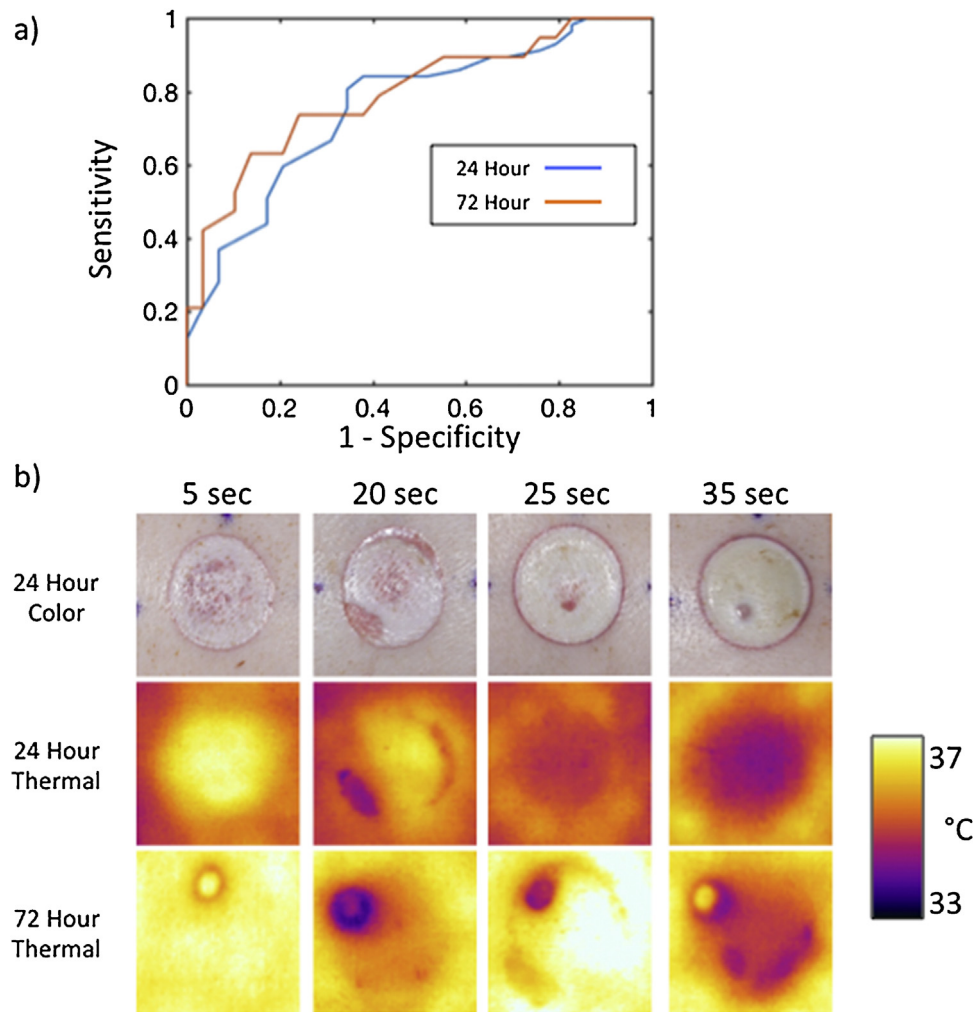


**Fig. 5 – a) ROC curves of thermography data from 24 and 72h after burn. b) Thermography images from 5, 20, 25 and 35 s burns at 24 and 72h after burn.**

sensitivity of 76% and a specificity of 74%. The positive and negative predictive values were 82% and 67% respectively. There was no statistically significant difference between the classifying ability of the thermography values at 24 and 72h. An example of typical thermography images collected are shown in Fig. 5b. At 24h, temperature within the superficial partial burn (5s) regions are higher than unburned tissue. The 20s burn demonstrated similar temperature to unburned tissue at 24h, and both the 25 and 35s burns were lower in temperature than unburned tissue at 24h. At 72h, the temperature within the 5s burn was similar to unburned tissue. The 20s, 25s and 35s burns had lower temperatures than unburned tissue at 72h. The temperature measurements of the unburned regions during 72h measurements were higher than that recorded at 24h.

### 3.5. SFDI measured reduced scattering changes

The averaged reduced scattering coefficient, ( $\mu_s'$ ) values at 24 and 72h were used to create the ROC shown in Fig. 6a. The AUC of the 24h  $\mu_s'$  values was 0.90, while the AUC of the 72h AUC values was

0.91. Both values were statistically significant ( $p < 0.001$ ). After choosing a threshold of  $1.23\text{mm}^{-1}$ , the overall accuracy off the 24h perfusion values 85% (41/48) with a sensitivity of 93% and a specificity of 74%. The positive and negative predictive values were 84% and 88% respectively. The 72h  $\mu_s'$  values also had an overall accuracy of 85% (correct classification of 41/48) with a sensitivity of 83% and a specificity of 90%. The positive value was 92% and the negative predictive value was 77%. There was no statistically significant difference between the classifying ability of the  $\mu_s'$  values at 24 and 72h. Fig. 6b shows images of  $\mu_s'$  typical perfusion images at 24h and 72h.

### 3.6. Summary

A summary of the statistics for all the imaging modalities at 24 and 72h are shown in Table 3.

A comparison of the classifiers at 24h, as a function of measurement modality, using McNemar's test, showed a statistically significant difference when comparing SFDI with LSI and thermal imaging. Additionally, there was a statistically significant difference when comparing clinical analysis with

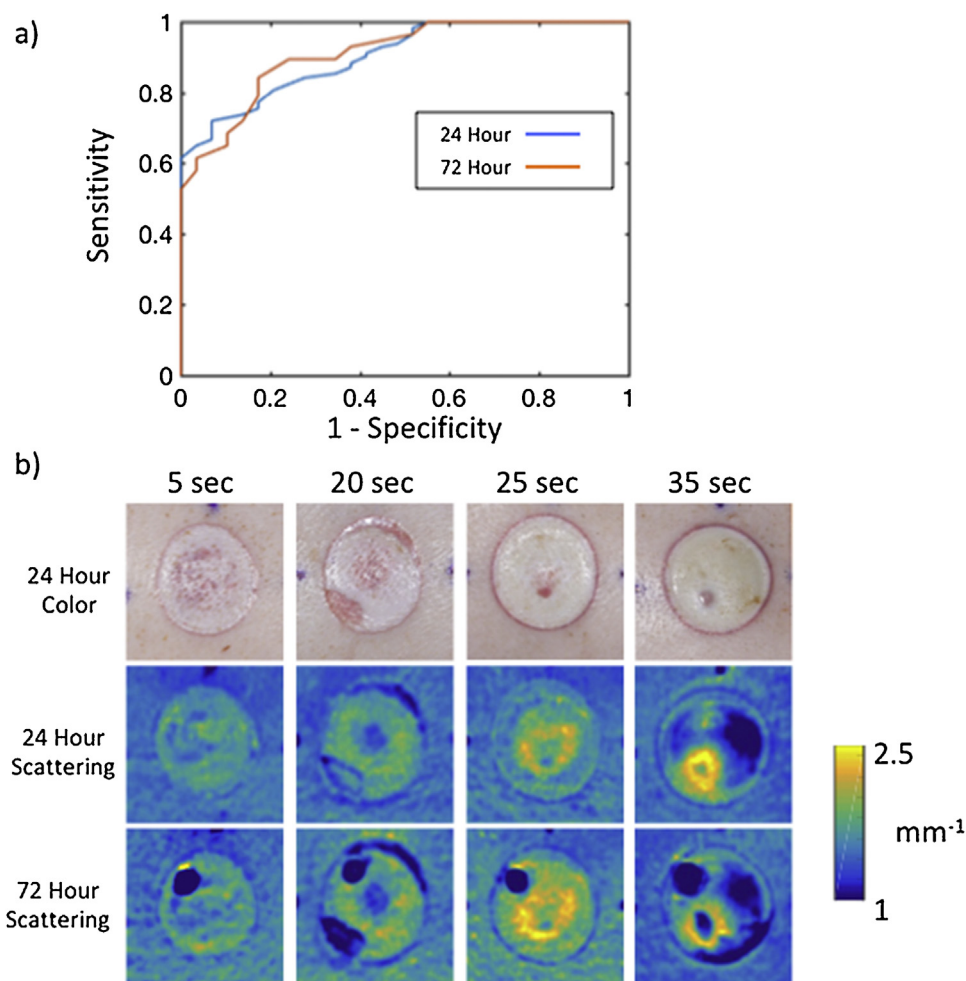


Fig. 6 - a) ROC curves of SFDI scattering data from 24 and 72h after burn. b) Images of reduced scattering at 659 nm from 5, 20, 25 and 35s burns at 24 and 72h after burn.

LSI and thermal imaging. Results for all modalities are shown in Table 4.

#### 4. Discussion

##### 4.1. Histological assessment

As one of the gold standards for determining burn severity [24,25], histology illustrates detailed changes within tissue

after the burn wound is created, as seen in Fig. 3. While histology represents a conventional and relatively objective means to determine burn depth, taking and processing biopsies is a time consuming process. In addition, it is an extremely invasive procedure which is not practical from a clinical standpoint. Furthermore, the relatively small region of tissue sampled by histology is likely not representative of the severity of the entire burn region, which in our experience may be several hundreds of square centimeters in extent. Indeed, spatial heterogeneity of burns are well documented, even in

Table 3 – Summary of statistics obtained using different measurement modalities.

	Accuracy (%)	Sensitivity (%)	Specificity (%)	PPV (%)	NPV (%)
Clinical assessment (24h)	83	100	58	78	100
LSI (24h)	75	66	90	91	63
Thermography (24h)	73	66	84	86	62
SFDI (24h)	85	93	74	84	88
Clinical assessment (72h)	85	100	63	81	100
LSI (72h)	83	100	58	78	100
Thermography (72h)	75	76	74	82	67
SFDI (72h)	85	83	90	92	77

**Table 4 – McNemar’s test p-values for comparing modalities at 24h.**

	Clinical	LSI	Thermography	SFDI
Clinical	N/A	<0.001*	<0.001*	0.07
LSI	<0.001*	N/A	1.00	0.003*
Thermography	<0.001*	1.00	N/A	0.004*
SFDI	0.07	0.003*	0.004*	N/A

\* Denotes  $p < 0.05$ .

controlled studies like the current one that aim for homogeneous sounds (as seen in scattering values in Fig. 6b). The rapid collagen changes associated with the zone of coagulation within burns may explain why techniques like SFDI, which is sensitive to structural changes [21,22], may provide information as early as a few hours after burn [23]. Physiological changes such as perfusion and temperature typically occur 48–72h after burn [3].

#### 4.2. Laser Speckle Imaging

Other investigators have found that LSI technology becomes compelling as a tool with which to assess burn wound severity in the 48–72h time window [29]. When comparing the accuracy of clinical observation and laser Doppler imaging techniques, time points of 24h and 72h have been used to highlight the advantage of laser Doppler imaging over clinical assessments [3]. The 24h time point provides the benefit of being clinically relevant in terms of when patients often present to clinical staff for burn wound treatment. Commercialized LSI devices have frequently been used to study burns in animal models and also in a clinical setting on human patients [30]. They have typically demonstrated an ability to categorize which burns benefit from surgical intervention more accurately than clinicians [3,8,29]. LSI typically has an accuracy of about 80% 24h after the burn that increases to approximately 95% at 72h after the burn [3]. While we saw an accuracy of 75% using LSI at 24h, there was not a significant increase in accuracy at 72h. Additionally, as seen in Fig. 4b, there was no increase in perfusion for burns that do not receive intervention. This increase is well documented in the clinical setting and likely leads to the increased classification accuracy at the later time points. It is possible that this response is delayed in the animal model studied. Other studies that have focused on animal models have similarly seen decreased perfusion that can last for 7–14days depending on burn severity. This delayed perfusion response could help explain the lack of a larger increase in diagnostic accuracy at 72h. The same study investigated the classification ability of LSI and reported the AUC of perfusion measurements taken 1h after burn to be 78%, which was similar to the AUC of 79% for our 24h measurements [31].

#### 4.3. Thermal imaging

Thermal imaging was able to classify burns at 24 and 72h using temperature measurements, but ultimately performed worse than clinical assessment, LSI and SFDI. A 2017 study recently

compared real-time clinical assessments and passive thermal imaging of burns on clinical patients[8]. The study found that thermal imaging at 24h was 56% accurate, and at 72h was 71% accurate. Real-time clinical assessments outperformed thermal imaging and was 88% accurate at 24h. We found similar results in our study as real-time clinical assessments (83% accuracy) outperformed thermal imaging at 24h (73% accuracy) and 72h (75% accuracy).

#### 4.4. SFDI

In terms of overall accuracy, SFDI (85%) was the only imaging modality to perform better than clinical assessment (83%) at 24h. It also performed significantly better than LSI and thermal imaging at classifying burns by whether they would benefit from surgical intervention. While previous work using SFDI in rat burn experiments [23] as well as pig burn experiments [21,22,32] have focused on the ability to distinguish different categories of burns, here we have focused on directly comparing it to clinical observation along with other popular imaging modalities for burn care. A key difference between SFDI and the other imaging modalities is that the reduced scattering coefficient changes are largely in response to changes in tissue structure that occur immediately after the burn, whereas LSI and thermal imaging rely on perfusion changes that typically occur days later. While early measurements from all devices perform well, LSI and thermal imaging did not exceed what could be done by clinical analysis alone. SFDI outperformed the other imaging modalities and has the added benefit of measuring multiple parameters meaning future work can focus on optimizing SFDI measurements.

#### 4.5. Summary

In this experiment, 16 burns were created on 3 pigs yielding 48 burns that were treated as independent data points. While the different burn wounds in an individual pig may not be completely independent of each other, this assumption is necessary in order to develop enough data points for any significant analysis similar to what other groups have done [13,31,33–36]. Based on the size of the burn wounds relative to the total body surface area (~1%) there should be no systemic effects and the distance between each wound (~3cm) should ensure that these wounds represent unique samples from a diagnostic imaging standpoint.

While we have examined the results from these imaging techniques in a controlled experiment, it is important to consider the strengths and weaknesses of each technique in a clinical setting. Laser speckle imaging techniques have the advantage of being well established for examining burn wounds based on a long history that began with laser Doppler techniques that evolved into laser Doppler imaging [37]. LSI has considerably reduced acquisition times from previous scanning laser Doppler techniques. This increase in speed reduces movement artifacts and enables real time feedback to clinicians. The clinical accuracy of LSI over clinical observation is well documented [29], but the expense of current commercial systems does limit widespread use [5]. Thermal imaging systems also have fast acquisition times and can provide real

time feedback to clinicians. Hand-held systems have recently been commercialized and these are relatively inexpensive [9]. However thermal imaging can be very sensitive to fluctuations in ambient temperature [10] and studies that have directly compared laser Doppler techniques and thermal imaging have found that laser Doppler can be more accurate in terms of categorizing burn severity [8]. SFDI is a newer technology and commercial realization of devices is in early stages. Thus, interfaces and data collection procedures, while appropriate for research studies, are still being refined to enable clinical data collection. SFDI collects a larger data set (multiple wavelength images at multiple spatial frequencies) than LSI or thermal imaging systems. This means that data acquisition can take longer (up to a minute at the current state of development employed here) and data analysis is still being refined in order to optimize the information content of the results. However the additional information provided by SFDI allows it to outperform the other systems in terms of burn assessment accuracy in these controlled experiments. Future studies have the potential to optimize the information content provided by SFDI in terms that are most relevant for burn wounds. This will enable reduction in data set sizes and thus shorter acquisition times that present only the most relevant data to clinicians.

## 5. Conclusion

SFDI, LSI and thermal imaging are all non-invasive modalities that according to the literature can help discriminate differences in burn severity and clinical decision making [1,8]. While new technologies have the capability to aid the decision making capabilities of burn clinicians, they must be tested in a controlled environment to gauge their efficacy. These techniques have been studied individually and sometimes comparatively in clinical and research settings, but here we present those modalities in relationship to clinical analysis in a controlled animal model in which burn severity has been verified using histological assessment. We found that SFDI was the only modality to have a diagnostic accuracy higher than clinical assessment.

## Acknowledgments

We gratefully acknowledge support from NIGMS grant R01GM108634 and the NIBIB, including P41EB015890 (A Biomedical Technology Resource). The content is solely the responsibility of the authors and does not necessarily represent the official views of the NIGMS, NIBIB or NIH. We also acknowledge the Arnold and Mabel Beckman Foundation. We would also like to thank Earl Steward for facilitating the animal work involved in this study.

## Conflict of interest

The authors have no financial interests or commercial associations that might pose or create a conflict of interest with the information presented in this article.

## REFERENCES

- [1] Peck MD. Epidemiology of burns throughout the world: part I: distribution and risk factors. *Burns* 2011;37:1087–100.
- [2] Shupp JW, Nasabzadeh TJ, Rosenthal DS, Jordan MH, Fidler P, Jeng JC. A review of the local pathophysiologic bases of burn wound progression. *J Burn Care Res* 2010;31:849–73.
- [3] Hoeksema H, Van de Sijpe K, Tondu T, Hamdi M, Van Landuyt K, Blondeel P, et al. Accuracy of early burn depth assessment by laser Doppler imaging on different days post burn. *Burns* 2009;35:36–45.
- [4] Burke-Smith A, Collier J, Jones I. A comparison of non-invasive imaging modalities: Infrared thermography, spectrophotometric intracutaneous analysis and laser Doppler imaging for the assessment of adult burns. *Burns* 2015;41:1695–707.
- [5] Kaiser M, Yafi A, Cinat M, Choi B, Durkin AJ. Noninvasive assessment of burn wound severity using optical technology: a review of current and future modalities. *Burns* 2011;37:377–86.
- [6] Krezdorn N, Limbourg A, Paprottka FJ, Konneker, Ipaktchi R, Vogt PM. Assessing burn depth in tattooed burn lesions with LASCA Imaging. *Ann Burns Fire Disasters* 2016;29:223–7.
- [7] Nguyen K, Ward D, Lam L, Holland AJ. Laser Doppler Imaging prediction of burn wound outcome in children: is it possible before 48h? *Burns* 2010;36:793–8.
- [8] Wearn C, Lee KC, Hardwicke J, Allouni A, Bamford A, Nightingale P, et al. Prospective comparative evaluation study of Laser Doppler Imaging and thermal imaging in the assessment of burn depth. *Burns* 2018;44:124–33.
- [9] Burmeister DM, Cerna C, Becerra SC, Sloan M, Wilmlink G, Christy RJ. Noninvasive techniques for the determination of burn severity in real time. *J Burn Care Res* 2017;38:e180–91.
- [10] Miccio J, Parikh S, Marinaro X, Prasad A, McClain S, Singer AJ, et al. Forward-looking infrared imaging predicts ultimate burn depth in a porcine vertical injury progression model. *Burns* 2016;42:397–404.
- [11] Paluchowski LA, Nordgaard HB, Bjorgan A, Hov H, Berget SM, Randeberg LL. Can spectral-spatial image segmentation be used to discriminate experimental burn wounds? *J Biomed Opt* 2016;21:101413.
- [12] Calin MA, Parasca SV, Savastru R, Manea D. Characterization of burns using hyperspectral imaging technique — a preliminary study. *Burns* 2015;41:118–24.
- [13] King DR, Li W, Squiers JJ, Mohan R, Sellke E, Mo W, et al. Surgical wound debridement sequentially characterized in a porcine burn model with multispectral imaging. *Burns* 2015;41:1478–87.
- [14] Chin MS, Babchenko O, Lujan-Hernandez J, Nobel L, Ignatz R, Lalikos JF. Hyperspectral imaging for burn depth assessment in an animal model. *Plast Reconstr Surg Global Open* 2015;3:e591.
- [15] Cuccia DJ, Bevilacqua F, Durkin AJ, Ayers FR, Tromberg BJ. Quantitation and mapping of tissue optical properties using modulated imaging. *J Biomed Opt* 2009;14:024012.
- [16] Cuccia DJ, Bevilacqua F, Durkin AJ, Tromberg BJ. Modulated imaging: quantitative analysis and tomography of turbid media in the spatial-frequency domain. *Opt Lett* 2005;30:1354–6.
- [17] Torabzadeh M, Park IY, Bartels RA, Durkin AJ, Tromberg BJ. Compressed single pixel imaging in the spatial frequency domain. *J Biomed Opt* 2017;22:30501.
- [18] Wilson RH, Crouzet C, Torabzadeh M, Bazrafkan A, Farahabadi MH, Jamasian B, et al. High-speed spatial frequency domain imaging of rat cortex detects dynamic optical and physiological properties following cardiac arrest and resuscitation. *Neurophotonics* 2017;4:045008.
- [19] Ponticorvo A, Taydas E, Mazhar A, Scholz T, Kim HS, Rimler J, et al. Quantitative assessment of partial vascular occlusions in

- a swine pedicle flap model using spatial frequency domain imaging. *Biomed Opt Express* 2013;4:298-306.
- [20] Yafi A, Vetter TS, Scholz T, Patel S, Saager RB, Cuccia DJ, et al. Postoperative quantitative assessment of reconstructive tissue status in a cutaneous flap model using spatial frequency domain imaging. *Plast Reconstr Surg* 2011;127:117-30.
- [21] Ponticorvo A, Burmeister DM, Yang B, Choi B, Christy RJ, Durkin AJ. Quantitative assessment of graded burn wounds in a porcine model using spatial frequency domain imaging (SFDI) and laser speckle imaging (LSI). *Biomed Opt Express* 2014;5:3467-81.
- [22] Burmeister DM, Ponticorvo A, Yang B, Becerra SC, Choi B, Durkin AJ, et al. Utility of spatial frequency domain imaging (SFDI) and laser speckle imaging (LSI) to non-invasively diagnose burn depth in a porcine model. *Burns* 2015;41:1242-52.
- [23] Nguyen JQ, Crouzet C, Mai T, Riola K, Uchitel D, Liaw LH, et al. Spatial frequency domain imaging of burn wounds in a preclinical model of graded burn severity. *J Biomed Opt* 2013;18:66010.
- [24] Watts AM, Tyler MP, Perry ME, Roberts AH, McGrouther DA. Burn depth and its histological measurement. *Burns* 2001;27:154-60.
- [25] Thomsen S. Pathologic analysis of photothermal and photomechanical effects of laser-tissue interactions. *Photochem Photobiol* 1991;53:825-35.
- [26] Boylan A, Martin CJ, Gardner GG. Infrared emissivity of burn wounds. *Clin Phys Physiol Meas* 1992;13:125-7.
- [27] Ayers F, Grant A, Kuo D, Cuccia DJ, Durkin AJ. Fabrication and characterization of silicone-based tissue phantoms with tunable optical properties in the visible and near infrared domain. *Proc Spie* 2008;6870.
- [28] Fluss R, Faraggi D, Reiser B. Estimation of the Youden Index and its associated cutoff point. *Biom J* 2005;47:458-72.
- [29] Shin JY, Yi HS. Diagnostic accuracy of laser Doppler imaging in burn depth assessment: Systematic review and meta-analysis. *Burns* 2016;42:1369-76.
- [30] Lindahl F, Tesselaar E, Sjoberg F. Assessing paediatric scald injuries using Laser Speckle Contrast Imaging. *Burns* 2013;39:662-6.
- [31] Ganapathy P, Tamminedi T, Qin Y, Nanney L, Cardwell N, Pollins A, et al. Dual-imaging system for burn depth diagnosis. *Burns* 2014;40:67-81.
- [32] Mazhar A, Saggese S, Pollins AC, Cardwell NL, Nanney L, Cuccia DJ. Noncontact imaging of burn depth and extent in a porcine model using spatial frequency domain imaging. *J Biomed Opt* 2014;19:086019.
- [33] Heredia-Juesas J, Thatcher JE, Lu Y, Squiers JJ, King D, Fan W, et al. Burn-injured tissue detection for debridement surgery through the combination of non-invasive optical imaging techniques. *Biomed Opt Express* 2018;9:1809-26.
- [34] Gaines C, Poranki D, Du W, Clark RA, Van Dyke M. Development of a porcine deep partial thickness burn model. *Burns* 2013;39:311-9.
- [35] Sowa MG, Leonardi L, Payette JR, Cross KM, Gomez M, Fish JS. Classification of burn injuries using near-infrared spectroscopy. *J Biomed Opt* 2006;11:054002.
- [36] Gnyawali SC, Barki KG, Mathew-Steiner SS, Dixith S, Vanzant D, Kim J, et al. High-resolution harmonics ultrasound imaging for non-invasive characterization of wound healing in a pre-clinical swine model. *PLoS one* 2015;10:e0122327.
- [37] Stewart CJ, Frank R, Forrester KR, Tulip J, Lindsay R, Bray RC. A comparison of two laser-based methods for determination of burn scar perfusion: laser Doppler versus laser speckle imaging. *Burns* 2005;31:744-52.